Separation Science Plus

WILEY-VCH

SSC plus

RESEARCH ARTICLE

Stability Indicating High-Performance Liquid Chromatographic Method for the Assessment of Thermal Stability of Antitubercular Drug Combinations, and Characterization of Rifampicin–Isoniazid Adduct Impurity

Deepjyoti Das[1] | Pragati Sinha[1] | Pothuraju Naresh[1] | Sombir Saharan[2] | Azger Dusthackeer VN[3] | Krishna VeniNagappan[4] | Vinod L. Gaikwad[2] | Ramalingam Peraman[1]

[1]Department of Pharmaceutical Analysis, National Institute of Pharmaceutical Education and Research (NIPER), Hajipur, Bihar, India | [2]Department of Pharmaceutics, National Institute of Pharmaceutical Education and Research (NIPER), Hajipur, Bihar, India | [3]ICMR-National Institute for Research in Tuberculosis (NIRT), Chennai, Tamil Nadu, India | [4]JSS College of Pharmacy, JSS Academy of Higher Education & Research, Ooty, Tamil Nadu, India

Correspondence: Ramalingam Peraman (drram@niperhajipur.ac.in; drramalingamp@gmail.com)

Received: 4 July 2025 | **Revised:** 17 December 2025 | **Accepted:** 23 December 2025

Keywords: 3-(isonicotinoylhydrazinomethyl) rifamycin | antitubercular activity | gradient high-performance liquid chromatography | stability-indicating | thermal stability

ABSTRACT

A stability indicating high-performance liquid chromatographic method was developed for the determination of the thermal stability of antitubercular drug combinations. The method separated the analytes and degradation products using a gradient elution of a mixture of ammonium formate buffer and methanol on a C_{18} column. The method demonstrated acceptable specificity, resolution, linearity, precision, and accuracy for isoniazid, pyrazinamide, and rifampicin. The method was robust against changes in %buffer composition (± 2%), flow rate (± 0.1 mL/min), and column temperature (± 2°C). The method demonstrated the thermal stability of each drug alone and their three and two-drug combinations at 70°C for 10 days. The developed method revealed that the %degradation of isoniazid and rifampicin was relatively higher in the isoniazid–rifampicin combination than in the isoniazid–rifampicin–pyrazinamide combination. On Days 5 and 10, the respective percentages of degradation of 69.17% and 74.79% were recorded for rifampicin in the isoniazid + rifampicin combination, while the percentages of degradation of 78.99% and 80.0% were observed for isoniazid in the isoniazid + rifampicin combination. The %degradation for isoniazid and rifampicin was higher by 1.5-2-folds in isoniazid–rifampicin than in isoniazid + rifampicin + pyrazinamide combinations. Overall, the anti-tuberculosis fixed-dose combination generated 14 degradation products (Impurities 1–14), among which Impurity 12 was the most prominent. Accordingly, Impurity 12 was characterized as 3-(isonicotinoylhydrazinomethyl) rifamycin by ultraviolet-visible-near infrared spectroscopy, Fourier transform infrared spectroscopy, Hydrogen-1 nuclear magnetic resonance, and liquid chromatography-high resolution mass spectrometry (mass-to-charge ratio 843.350 of M-H). Furthermore, it was identified as a reaction product of isoniazid and rifampicin, generated at elevated temperatures. The isolated impurity was screened against *Mycobacterium tuberculosis* $H_{37}Rv$ and was found to be inactive with a minimum inhibitory concentration of > 250 µg/mL. Then, this method was applied to detect the isoniazid–rifampicin reaction products in marketed tablets and stability samples from an *in-house* liposome formulation study.

Deepjyoti Das, Pragati Sinha, and Pothuraju Naresh contributed equally to this study.

1 | Introduction

Tuberculosis (TB) is the world's second most common infectious disease and causes the highest mortality [1]. Despite the antimicrobial drug resistance in antitubercular therapy due to the emergence of multidrug-resistant tuberculosis (MDR-TB) and extensively drug-resistant tuberculosis (XDR-TB), yet the first-line TB drug regimen plays a significant role in the management of TB [2]. To ensure patient compliance with therapy, fixed-dose combinations (FDCs) of tablet dosage forms are available in the market, which are composed of isoniazid 75 mg (INH), rifampicin 150 mg (RIF), pyrazinamide 400 mg (PYZ), and ethambutol 275 mg (ETB). These four drugs, FDC, are prescribed during the initial intensive phase of drug-sensitive TB, followed by two drugs, FDC of INH and RIF, for a period of four months as a continuous phase. These FDC dosage forms are known for a few advantages, including enhanced medication compliance, economic, low rate of drug-resistance re-emergence of TB [3–5]. However, this regimen is more toxic, and non-adherence may lead to the emergence of drug resistance and mortality.

However, the impurity profile of anti-TB FDCs was not explored, especially after the release of the ICH Q3A R2 and Q3B R2 documents [6]. Previous literature has demonstrated that the impurity profile of the FDC dosage form differs significantly from that of its respective single-component dosage forms [7]. For instance, the FDC of anti-TB drugs in tablet dosage form is known to produce new impurities due to possible chemical or physical interactions among INH, RIF, PYZ, and ETB. Indeed, WHO has reported an impurity in anti-TB FDC drugs resulting from a reaction between INH and RIF [8]. RIF facilitates the acetylation of INH by metabolic enzymes, after which the acetylated INH interacts with the hydrazone group of RIF to yield an adduct impurity [9]. In quality control, analytical challenges persist in assessing the stability of anti-TB FDC drugs. Few analytical methods have been reported for the multi-component analysis of anti-TB FDCs, including high-performance liquid chromatography with ultraviolet detection (HPLC-UV) [10–18], LC-MS/MS [16, 19–23], LC-NMR [24, 25], and capillary electrophoresis [26, 27] techniques. A focused review of reported stability-indicating HPLC methods for anti-TB FDCs [28, 29] revealed the formation of several impurities under stress degradation. However, the reported stability-indicating HPLC methods utilized buffers such as monobasic sodium phosphate and tetra-butylammonium hydroxide for gradient elution of analytes and impurities [30, 31]. Nevertheless, those methods were developed with long run times, high baseline drift, and poor resolution between analytes or analyte-impurities, especially low resolution between isoniazid and pyrazinamide [32–34]. Considering the marked availability of anti-TB regimens, we found no reliable HPLC study demonstrating the comparative thermal degradation profile of two combinations of anti-TB FDCs. In view of the above, this work has been planned to develop a new HPLC method using volatile buffers to demonstrate the thermal stability of two (INH + RIF) and three (INH + RIF + PYZ) anti-TB FDC combinations. Here, we investigated the suitability of ammonium formate and ammonium acetate in developing a new stability-indicating HPLC method for analyzing anti-TB FDC combinations. Furthermore, the performance of the developed method was tested on marketed anti-TB FDC dosage forms and in-house liposomal formulations.

2 | Material and Methods

2.1 | Chemicals, Standards, and Samples

HPLC grade acetonitrile and methanol solvents were purchased from Molekula SRL (India). Standard drugs, rifampicin (99.9%), isoniazid (98.98%), ethambutol (98.8%), pyrazinamide (99.1%), and ammonium formate (96.0%) were purchased from Sigma-Aldrich (India). All solutions and buffers were prepared using in-house ultra-pure water (Milli-Q purifying water system, Millipore, India). Laboratory glassware of Class A type (Indian Pharmacopoeia) was used in the preparation of standard solutions. The extra pure reagent $BaSO_4$ (99.99%) was used in a solid-state UV-Visible-NIR study. TLC grade silica gel, AR grade n-hexane, and ethyl acetate solvents were procured from TCI Chemicals, India.

2.2 | Instrumentation and Analytical Method Conditions

An Agilent 1200 LC system (Model no. 1260 Infinity II, India), comprising a quaternary pump, autosampler, and photodiode array detector, was utilized for the HPLC analyses. The software, Agilent HP Chem Station Version 3.2, was used for data acquisition and analysis. At a temperature of 25°C, the Inertsil ODS C18 column (250 × 4.6 mm, 5 μ particle size) from GL Sciences was employed for the separation of drugs and impurities. ETB was detected at 210 nm, while rifampicin, isoniazid, and pyrazinamide were detected at 254 nm. HPLC grade methanol was used as mobile phase B, while 200 mM ammonium formate buffer (pH adjusted to 6.2 with phosphoric acid) was used as Mobile Phase A. The process of gradient elution was as follows: at a 30-min gradient program; 0–15.0 min-A: 97%, B: 3%; 15.1–25.0 min-A: 10% B: 90%; 25.1–30.0 min-A: 97% B: 3% with a 20 µL injection volume, the flow rate was 1 mL/min.

2.3 | Preparation of Standard Solutions

Accurately about 10 mg of each RIF, INH, PYZ, and ETB was transferred into a 10 mL volumetric flask, dissolved with one-third volume of HPLC grade methanol, and the volume was made up to 10 mL (1000 µg/mL). Furthermore, 0.2, 0.4, 0.5, 0.6, 0.8, and 1.0 mL of each was diluted with 200 mM ammonium formate in water and methanol to 10 mL (20, 40, 50, 60, 80, and 100 µg/mL) for the method development and validation experiment.

2.4 | Thermal Degradation of Anti-TB FDC

Thermal degradation of anti-TB FDC combination was conducted for two different combinations, namely, two drugs combination (INH + RIF) and three drugs combination (INH + RIF + PYZ). Each 100 mg of the physical mixture of each combination was subjected to thermal stress at a temperature of 70°C in a hot air

oven. The sample aliquot (10 mg) was withdrawn at different time points that is, Day 0, 1, 5, and 10, and was analyzed under the optimized HPLC conditions. Each thermal stress sample chromatogram was compared with the blank and control (standard) for the identification of the number of degradation products. The peak area of INH, RIF, and PYZ was used to calculate the %degradation.

2.5 | Detection of Thermal Degradation by Ultraviolet-Visible-Near-Infrared Solid-State Analysis

Control samples of INH–RIF and INH–RIF–PYZ was comparatively analyzed using a UV-Visible-NIR spectrophotometer with a solid sample accessories (CORP.00619) (Shimadzu-3600i plus). $BaSO_4$ was employed as a diluent. All samples were analyzed at a sample-diluent ratio of 1:10. Samples were screened using a wavelength range from 200 to 3000 nm. The obtained spectra were processed for the first derivative using lab LabSolutions UV-Vis platform.

2.6 | Method Optimization and Separation of Anti-TB Drugs and Degradation Products

The method development was carried out on an Inertsil ODS-3 V C18 Column (250 mm × 4.6 mm, 5 μ) at ambient column temperature. The method optimization began with different trials (10 trials) by isocratic elution mode using different combinations of methanol and ammonium acetate (Trials 1–5)/ammonium formate (Trials 6–10) buffer. The pH was investigated over the range of 6.2–6.9. Based on the elution efficiency, the method was switched to gradient mode using the combination of methanol and ammonium formate (pH 6.2). In gradient elution, three different formate buffer strengths, 50, 100, and 200 mM were tested (Figures S1–S3). Finally, based on acceptable system suitability test (SST), we arrived at a 30-min gradient program as follows: 0–15.0 min-A: 97%, B: 3%; 15.1–25.0 min-A: 10% B: 90%; 25.1–30.0 min-A: 97% B: 3%. The flow rate was 1 mL/min. The respective retention times for INH, RIF, PYZ, and Ethambutol were 6.5 ± 0.2, 18.7 ± 0.2, 7.3 ± 0.2, and 3.9 ± 0.1 min, respectively. RIF was found to be eluted at 18.7 ± 0.2 and with acceptable resolution from thermal degradation products and matrix peaks. Noted that ethambutol was detected only at 210 nm due to its weak chromophore chemical structure.

2.7 | Method Validation

The method was validated in accordance with the International Council on Harmonisation (ICH) Q2 (R1) guidelines. The validation parameters included were specificity, linearity, precision, accuracy, limits of detection, limit of quantification, and robustness.

2.8 | Detection of Isoniazid–Rifampicin Adduct in Marketed Formulation

Twenty tablets of markedly available anti-TB FDC (manufactured by Lupin Ltd; Dose: 150 mg RIF, 75 mg INH, 400 mg PYZ, and 275 mg ETB) were ground into powder. A powder equivalent to precisely 15.0 mg of RIF, 7.5 mg of INH, 40.0 mg of PYZ, and 27.5 mg of ETB was added to a 100 mL volumetric flask containing 50 mL of Mobile Phase A. The mixture was then extracted under sonication for 20 min, after which the volume was made up to 100 mL with Mobile Phase B. The content was filtered using a 0.2 µm filter (Nylon) and analyzed under the optimized HPLC method conditions.

2.9 | Detection of Isoniazid–Rifampicin Adduct in *In-House* Liposomal Formulation

Based on the entrapment efficiency of the *in-house* liposomal formulation containing INH and RIF, a liposome lyophilized powder equivalent to 15.0 mg of RIF and 7.5 mg of INH was weighed and transferred to a 100 mL volumetric flask containing 50 mL of Mobile Phase A. The rest of the procedure was followed as per the previous section. A blank liposomal solution has been prepared in the same manner for specificity verification and impurity identification.

2.10 | Isolation and Characterization of Isoniazid–Rifampicin Reaction Product (Adduct)

The impurity was isolated using preparative TLC (1 mm thickness of silica gel G). The preparative TLC for the separation of INH–RIF reaction adducts was performed using a mobile phase consisting of 95% methanol and 5% chloroform, with two drops of 10% ammonia solution added. The separation was visualized under 254 and 365 nm. The separated bands were scrapped and extracted using MS-grade methanol and then crystallized. The purity of the isolated impurity was checked using HPLC analysis and identified by the spike method. Furthermore, the isolated impurity was structurally characterized using melting point, UV-Visible-NIR, FT-IR, ^{1}H NMR, and LC-MS/MS (ESI) spectral analysis.

2.11 | Antitubercular Activity of Isoniazid–Rifampicin Reaction Product

The isolated impurity, INH–RIF reaction product, was screened against *M. tuberculosis* H_{37}Rv using the micro broth dilution method (250–1.4 µg/mL). RIF (Sigma-Aldrich) was used as a reference compound at 1 µg/mL. The procedure for the determination of minimum inhibitory concentration (MIC) was as same as described in our previous reported literature [31].

3 | Results and Discussion

3.1 | Method Development

The literature revealed that very few HPLC methods were reported for the determination of stress stability of first-line anti-TB FDC drugs. The choice of detector and elution mode was found to be the most significant variation among the methods reported. It was reported that INH and RIF react to each other at elevated temperatures and produce an INH–RIF adduct product as an impurity. This impurity is known as 3-(isonicotinoylhydrazinomethyl) rifamycin with a molecular mass

of m/z 843.350. At this juncture, our literature search did not yield any suitable HPLC methods for stability indicating the purpose of anti-TB FDC drugs, particularly in addressing the formation of INH–RIF adduct impurities. Therefore, this work was designed to develop a new stability indicating method for the simultaneous analysis of anti-TB drugs and to characterize the formation of specified thermal impurity at an elevated temperature. We designed to conduct thermal degradation in two different combinations namely, two drug combinations (INH + RIF) and three drug combinations (INH + RIF + PYZ). To separate the drugs and their impurities, we used ammonium acetate and ammonium formate buffers, which were not explored previously.

Initially, different trials (10 trials) were conducted using the isocratic mode. In this isocratic mode, a combination of methanol and ammonium acetate (Trial 1–5)/formate (Trail 6–10) buffer (pH 6.2–6.9) was used by varying the composition of the buffer from 20% to 95%. These trials revealed that the ammonium formate buffer afforded the characteristic elution of INH and PYZ, but not RIF. Further, we noticed that the resolution between INH and PYZ was low. However, due to the higher strength of the acetate buffer, the retention time was not precise and the baseline drift was very high.

Next, we switched to gradient mode using the combination of methanol and ammonium formate (pH 6.2). In gradient elution, three different formate buffer strengths 50, 100, and 200 mM were tested. Comparing the chromatograms, we found that the elution of INH and RIF was good with an acceptable plate number at 200 mM. We found that the peak shape of INH was affected if the strength of the formate buffer was less than 100 mM. For PYZ, the peak shape was good only with pH 6.2 (Figure 1A). Accordingly, we arrived a 30-min gradient program as; 0–15.0 min-A: 97%, B: 3%; 15.1–25.0 min-A: 10% B: 90%; 25.1–30.0 min-A: 97% B: 3% for elution of INH, RIF, PYZ, and ETB with respective retention time of 6.5 ± 0.2, 18.7 ± 0.1, 7.3 ± 0.2, and 3.9 ± 0.2 min. Then, the method was verified for the separation of thermal degradants from drugs. RIF was found to be eluted at 18.3 ± 0.1 min and with acceptable resolution from thermal degradation products and matrix peaks (Figure 1B). The developed method detected six impurities for INH + RIF and eight impurities for INH + RIF + PYZ combinations. All impurities were well separated from the drugs. Noted that ethambutol was detected only at 210 nm due to its very weak chromophore system, and its retention was well separated from other analytes. Considering the method's objective to detect INH–RIF reaction products, the method was monitored at 254 nm. The method validation was excluded for ethambutol, as it was not detected at 254 nm, and for the reason that 210 nm showed very high baseline drift and noise. The final method conditions and SST parameters are listed in Table 1.

3.2 | Results of Method Validation

The method validation was conducted as per ICH Q2 (R1) guidelines and the results are depicted in Table 2.The validation parameters included specificity, linearity, accuracy, precision, limits of detection (LOD), limits of quantification (LOQ), and a SST. The specificity of the method was tested using a blank as mobile phase, degraded samples, and control samples. No co-elution was detected along with INH, RIF, and PYZ and their peak purity was > 99% at 254 nm. A total of 14 degradation products (Impurity 1–14) has been detected by this developed method, amongst Impurity 12 (18.4 min), was found to be very prominent and was identified as an INH–RIF reaction product through further isolation and characterization. Overall, peaks were well separated from each other and from buffer/blank interference. The purity angle is less than the purity threshold, which ascertained the purity of the eluted peak. The linearity of the method was established for each drug at a concentration range between 20 and 100 µg/mL. The regression coefficient (R^2) values of 0.9945, 0.9980, 0.9985, and 0.9516 were obtained for RIF, INH, PYZ, and ETB, respectively (Figures S6–S9; Tables S1–S4). Considering the very low peak response of ETB and low regression value ($r^2 < 0.9031$), even at 210 nm, ETB was eliminated from the method validation. The precision and accuracy were evaluated throughout the linearity at three levels: 20, 60, and 100 µg/mL (Figures S11–S15). The %RSD for repeatability (< 1.0%) and inter-day precision (< 1.7%) was less than 2%. Thus, it indicated the acceptable precision of the method. The accuracy of the method was evaluated through recovery studies at three levels: 80%, 100%, and 120% by the spike procedure. The recovery ranges were 98.38%–99.78%, 97.58%–102.69%, and 99.48%–102.94%, respectively, for RIF, INH, and PYZ. LOD and LOQ were calculated from the slope of the regression equation and standard deviation. The LOD and LOQ values for RIF, INH, and PYZ were 0.2000, 0.0160, and 0.0057 µg/mL and 0.6600, 0.5280, and 0.0188 µg/mL, respectively. The robustness of the method was evaluated for small variations in three method variables: mobile phase (± 2%), column temperature (± 2°C), and flow rates (± 0.1 mL/min). The robust experiments showed an acceptable %RSD for RIF, INH, and PYZ indicating that these method variables do not cause any substantial changes in the observed peak area. However, an alteration in retention time was observed with a change in flow rate, which may be due to a change in flow velocity that affects the relative rate of analyte migration in the column. Overall, the %RSD remained acceptable under all circumstances.

3.3 | Detection of Thermal Degradation by Ultraviolet-Visible-Near-Infrared Solid-State Analysis

UV-Visible-NIR spectra revealed a significant change in the characteristic bands observed for a thermally degraded sample compared to a control sample. The characteristics of the %reflectance band observed for the INH–RIF control were 2970, 2930, 2853, 2759, 2720, 2679, 2617, 2575, and 2370 nm. The characteristics of the %reflectance band observed for the INH–RIF–PYZ control were 2969, 2922, 2874, 2805, 2776, 2694, 2670, 2489, 2467, 2352, 2289, and 2242 nm. On the Day 10, the NIR spectra of degraded INH–RIF showed distinct bands of 2972, 2870, 2785, 2675, 2639, 2613, 2605, 2559, 2547, 2499, 2398, 2328, and 2268 nm. Similarly, NIR spectra of degraded INH–RIF–PYZ showed distinct bands at 2937, 2882, 2838, 2810, 2688, 2650, 2604, 2547, 2477, 2380, 2328, 2303, 2220, and 2164 nm. The overlay of the first derivative NIR spectra of the control and degraded sample (Day 10) showed a significant difference in %reflectance characteristics, as shown in Figure S5A,B.

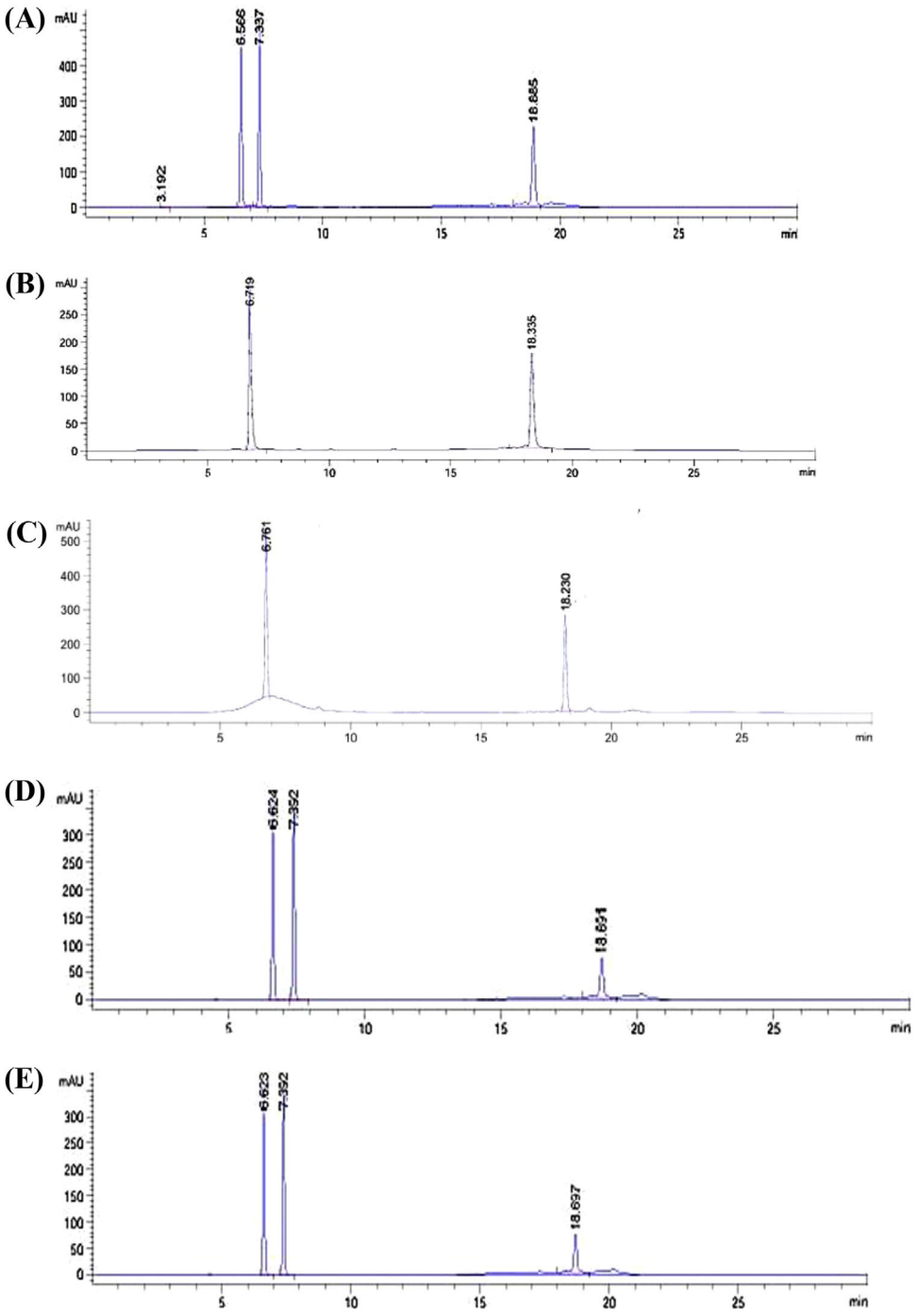

FIGURE 1 | Representative HPLC chromatograms for the quantification of isoniazid (INH), rifampicin (RIF), pyrazinamide (PYZ), and ethambutol HCl at 1000 μg/mL on a C18 column. (A) Optimized HPLC chromatograms of all analytes; (B) thermal degradation profile of INH + RIF on Day 5; (C) thermal degradation profile of INH + RIF on Day 10; (D) thermal degradation profile of INH + RIF + PYZ on Day 5; and E) thermal degradation profile of INH + RIF + PYZ on Day 10.

3.4 | Thermal Degradation Profile of Anti-TB Fixed Dose Combinations

The thermal degradation profile of the physical mixture of anti-TB FDC combinations is shown in Table 3 and Table S6, and the typical chromatograms are depicted in Figure 1B–E. A thermal degradation procedure was employed to solidify the powder mix for two combinations, namely, INH + RIF and INH + RIF + PYZ, at 70°C for 10 days. The HPLC analysis of the samples was carried out on Days 0 (control), 1, 5, and 10. There was no or negligible degradation observed on Day 1, but degradation was significant on Days 5 and 10. The total %degradation of INH in the INH + RIF combination was 78.9% and 80.0% on the 5th and 10th day, whilst RIF degraded to 69.1% and 74.7%, respectively. In INH + RIF + PYZ, the respective %degradation of 34.1 and 41.1% for INH, and 37.0% and 67.9% were recorded for RIF on Days 5 and 10. The %degradation of INH and RIF in the presence and absence of PYZ was significantly varied,

TABLE 1 | Final method conditions, system suitability test (SST) parameters for the optimized HPLC method.

Parameters	Rifampicin	Isoniazid	Pyrazinamide	Ethambutol HCL
Chromatographic column	Inertsil ODS-3 V C_{18} Column			
Column	250 × 4.6 mm, 5 µm			
Column temperature	25°C			
Mobile phase	A: 200 mM ammonium formate in water (pH 6.9); B: 100% methanol;			
Gradient elution	0–15.0 min: A: 97%, B: 3% 15.1–25.0 min A: 10% B: 90%; 25.1–30.0 min: A: 97% B: 3%			
Flow rate	1 mL/min			
Detection/wavelength	254 nm, 210 nm			
Run time	30 min			
Injection volume	20 µL			
Injection mode	Auto-sampler			
Theoretical plate	3400	2600	3000	3100
Retention time t_R ($n = 3$)	18.7 ± 0.1	6.5 ± 0.2	7.3 ± 0.2	3.9 ± 0.2
Tailing factor	1.15	1.1	1.07	1.5
Resolution from Rs/matrix	—	> 4	> 3	> 2
Flow rate accuracy ($n = 3$)	RSD: 0.42%			
Injection precision ($n = 3$)	RSD: 0.03%			

TABLE 2 | Method validation results for the optimized HPLC method.

Parameters		Rifampicin	Isoniazid	Pyrazinamide
Specificity		Pass peak purity > 99%	Pass peak purity > 99%	Pass peak purity > 99%
Linearity ($n = 3$)		20–100 µg/mL	20–100 µg/mL	20–100 µg/mL
Regression coefficient		0.9945	0.9980	0.9985
Intra-day precision (%RSD) ($n = 3$)	20 µg/mL	0.46	0.63	0.41
	60 µg/mL	0.87	0.91	0.80
	100 µg/mL	0.61	0.85	0.92
Inter-day precision ($n = 3$) (%RSD)	20 µg/mL	1.23	1.48	1.17
	60 µg/mL	1.69	1.04	1.04
	100 µg/mL	1.28	1.31	1.26
Accuracy ($n = 3$)	80 % level	98.38%	97.58%	102.94%
	100% level	98.82%	98.00%	97.95%
	120% level	99.78%	102.69%	99.48%
LOD (µg/mL)		0.20	0.0160	0.0057
LOQ (µg/mL)		0.66	0.528	0.0188
Robustness (% t_R RSD)		0.1	6.1	5.5
Flow rate (± 0.1 mL/min)		0.03	3.2	2.5
% Aqueous (± 2%)		0.3	1.1	0.7
Column Temp. (± 2°C)				

TABLE 3 | Percentage degradation data of INH and RIF under thermal degradation of INH + RIF + PYZ and INH + RIF combination and Impurity 12.

Day	INH + RIF combination (70°C)				INH + RIF + PYZ combination (70°C)			
	Total impurity	t_R (impurity) m/z 845	%Degradation (RIF)	%Degradation (INH)	Total impurity	t_R (impurity) m/z 845	%Degradation (RIF)	%Degradation (INH)
0	0	—	0	—	0	—	0	—
1	0	—	—	—	0	—	—	—
5	9	18.4 ± 0.1	69.17	78.99	12	18.4 ± 0.1	37.01	34.11
10	9	18.4 ± 0.1	74.79	80.0	12	18.4 ± 0.1	67.93	41.05

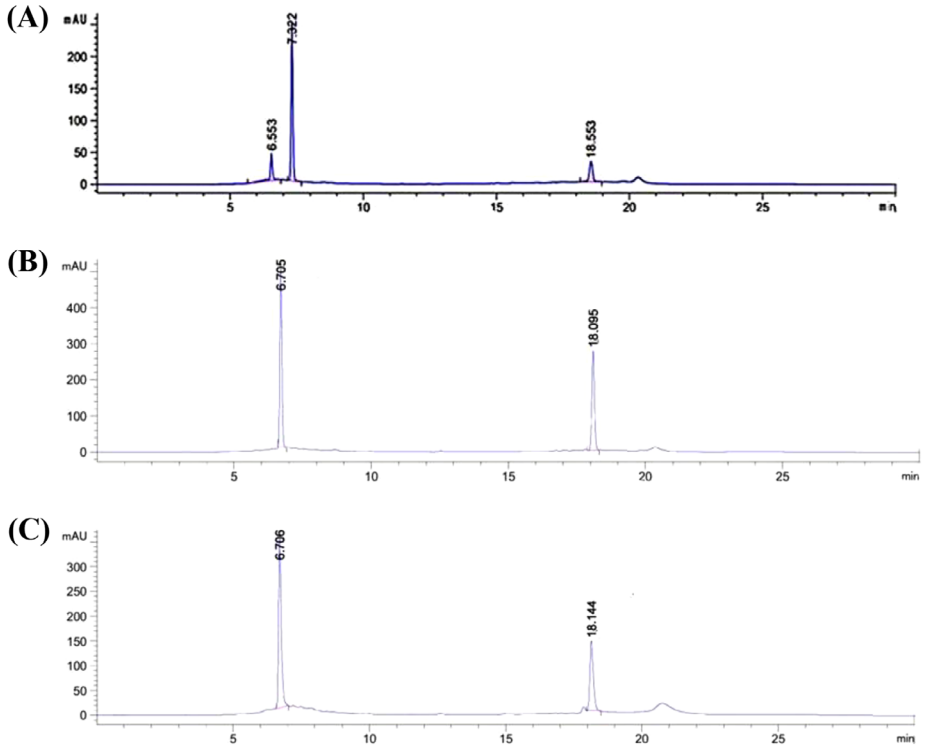

FIGURE 2 | Comparative data of degradation products INH + RIF + PYZ and INH + RIF combination under thermal stress on Day 5 and 10.

and noted that the %degradation of both drugs was found to be low in the presence of PYZ. On the 10th day, the %degradation of INH was high by 2-fold higher in the INH + RIF + PYZ combination as compared to INH + RIF. It indicated the significant role of PYZ in the degradation profile of INH and RIF.

Overall, the thermal degradation of anti-TB FDC at 70°C produced a total of 14 degradation products (Impurities 1–14) (Figure 2). Among them, Impurity 12 was the most abundant impurity, while the rest were minor impurities. INH + RIF combination produced nine (Impurity 4, 7, 8, 9, 10, 11, 12, 13, 14) and nine (Impurity 4, 6, 8, 9, 10, 11, 12, 13, 14) impurities at Days 5 and 10, respectively. Impurity 6 was detected only at Day 10. Similarly, the INH + RIF + PYZ combination produced a total of 12 impurities at both Days 5 and 10. It was noted that Impurities 5 and 7 were detected only on the fifth day. Similarly, Impurities 1 and 6 were detected only at Day 10. The impurity growth was found to be consistent with respect to their peak area. Among these, a total of eight impurities (Impurities 4, 8, 9, 10, 11, 12, 13, and 14) were the commonest impurities in both combinations at all time points. Noted, that Impurities-1, 2, 3, 5, and 7 are detected only in INH + RIF + PYZ. In PDA detection, we observed prominent degradation products at 17.7 ± 0.05 min, with a characteristic UV spectrum similar to that of both INH and RIF. It was inferred that the %degradation of both INH and RIF was not only due to decomposition but also due to the reaction between INH and RIF at high temperatures. This is in agreement with the previous literature and reported specified impurity with m/z of 843.36.

3.5 | Method Performance in the Detection of Isoniazid–Rifampicin Adduct Impurity in Drug Products

Upon successful completion of method validation, the method was used to determine the assay value of marketed formulations

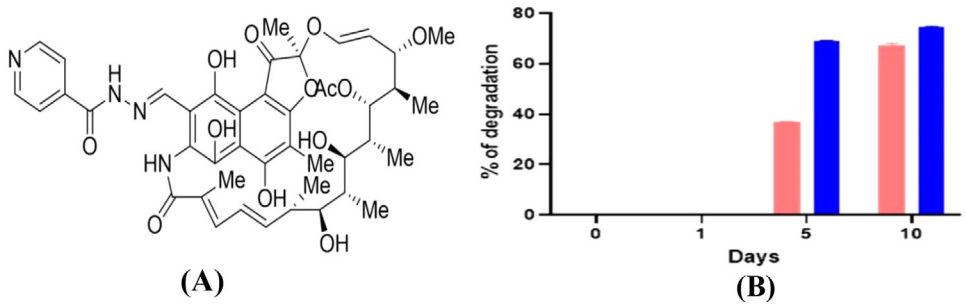

FIGURE 3 | A typical chromatograms of biological *in-house* samples at a concentration of 1000 μg/mL, including: (A) the marketed fixed-dose combination containing rifampicin (RIF), isoniazid (INH), pyrazinamide (PYZ), and ethambutol HCl; (B) the liposomal nanoformulation of RIF and INH; and (C) the INH–PLGA nanoparticle formulation.

TABLE 4 | Performance of the developed HPLC method in the detection of Impurity 12 (INH–RIF reaction product) and active content analysis in the formulation.

S. no.	Target formulation	Content			INH–RIF reaction product (Impurity 12)	Remarks
		INH	RIF	PYZ		
1	Marketed tablets -I	99.0%	98.3%	94.9%	No	Pass
2	Marketed tablets-II	98.5%	98.7%	93.1%	No	Pass
3	INH/RIF liposome (45°C)	65.8%	75.0%	—	Yes	Fail
4	INH/RIF liposome (45°C)	52.0%	64.2%	—	Yes	Fail
5	INH–PLGA nano-particle	42.0%	—	—	—	—

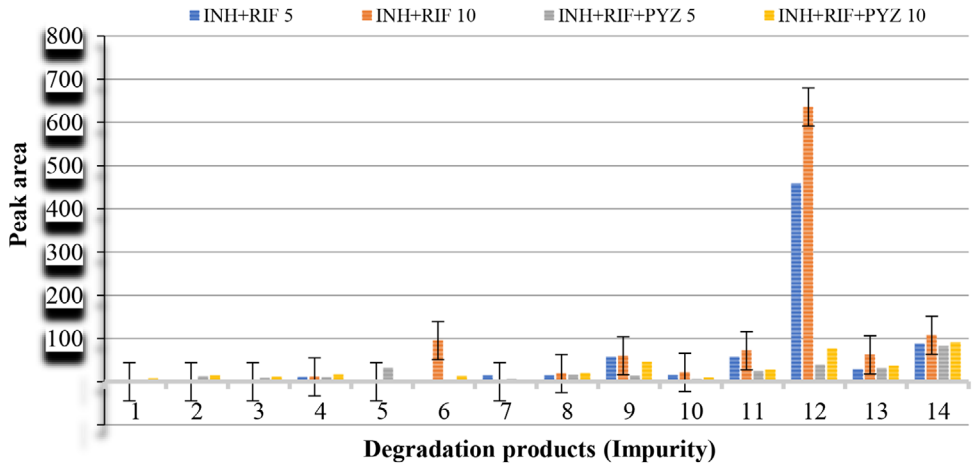

FIGURE 4 | (A) Chemical Structure of Impurity 12 (INH + RIF adduct impurity); and (B) levels of Impurity 12 detected in INH + RIF (Blue), and INH + RIF + PYZ (Red) at Day 5 and 10.

(Figure 3A) and to estimate the content of INH in the in-house formulation loaded PLGA nanoparticles (Figure 3C). In addition, the technique was employed to detect the formation of thermal impurities, namely, INH–RIF, in the liposomal formulation (co-loaded with lecithin) of both solution and lyophilized formulations (Figure 3B). The results were satisfactory in terms of theoretical loading and product specifications. The results are demonstrated in (Table 4).

3.6 | Isolation and Identification of Isoniazid–Rifampicin Adduct Impurity

The impurity, INH–RIF reaction product (Figure 4A) was isolated using preparative TLC. The impurity was isolated using a mobile phase consisting of 95% methanol and 5% chloroform, with two drops of a 10% ammonia solution added. The impurity was found to be colored and showed an R_f value of 0.88 and it seems to be less

polar than RIF. The isolated impurity was characterized using UV, IR, LC-MS/MS, and H^1-NMR (Figures S4A–C, and S16–S18). The overlay UV-Visible spectra of the isolated impurity with INH and RIF inferred the presence of characteristic chromophores of RIF and INH.

3.7 | Antitubercular Activity of Isoniazid–Rifampicin Reaction Product

The isolated impurity was screened against *M. tuberculosis* $H_{37}Rv$ using the micro broth dilution method. The compound was screened at serial dilutions ranging from 250 to 1.4 μg/mL. The results revealed that the INH–RIF reaction product showed an MIC of more than 250 μg/mL. Thus, it concluded that this impurity will have a significant impact on the efficacy of anti-TB FDC drug products.

4 | Conclusion

The HPLC method developed for the simultaneous analysis of first-line antitubercular drugs can be able to detect the stability of two and three-drug combinations under thermal stress conditions. This method is the first of its kind, utilizing an ammonium formate buffer with a 30-min gradient elution of anti-TB drugs on a C18 column, and employing photodiode array detection at 210 and 254 nm. The method demonstrated acceptable validation results. This piece of work characterized the most common impurity, 3-(isonicotinoylhydrazinomethyl) rifamycin as INH–RIF adduct impurity. The antitubercular screening of this adduct impurity revealed that it was inactive, even at a concentration of 250 μg/mL, against *M. tuberculosis* $H_{37}Rv$. This method also demonstrated acceptable performance in the assay of INH, RIF, and PYZ, as well as the detection of INH–RIF adduct impurity in marketed tablet dosage forms and *in-house* liposome formulations.

Author Contribution

Deepjyoti Das: sample preparation, stress degradation, instrument handling (HPLC), impurity isolation. **Pragati Sinha**: sample preparation, stress degradation, instrument handling (HPLC), impurity isolation. **Pothuraju Naresh**: method optimization, validation interpretation, literature collection, compilation, design of figures, and tables. **Sombir Saharan:** sample preparation. **Azger Dusthackeer VN**: antitubercular activity**. Vinod L Gaikwad**: liposomal formulation and stability studies. **Krishna VeniNagappan**: final editing and interpretation. **Ramalingam Peraman**: method development, validation, final editing, conceptualization, data interpretation, conclusions.

Acknowledgments

Authors are thankful to the Department of Pharmaceuticals, Ministry of Chemicals and Fertilizers, Govt. of India for the provided facilities.

Conflicts of Interest

The authors declare no conflicts of interest.

Data Availability Statement

All data generated during this study are included, along with a Supporting Information file in this published article.

References

1. A. Navarro-Flores, J. E. Fernandez-Chinguel, N. Pacheco-Barrios, D. R. Soriano-Moreno, and K. Pacheco-Barrios, "Global Morbidity and Mortality of Central Nervous System Tuberculosis: A Systematic Review and Meta-Analysis," *Journal of Neurology* 269, no. 7 (2022): 3482–3494, https://doi.org/10.1007/s00415-022-11052-8.

2. K. Chowdhury, R. Ahmad, S. Sinha, S. Dutta, and M. Haque, "Multidrug-Resistant TB (MDR-TB) and Extensively Drug-Resistant TB (XDR-TB) Among Children: Where We Stand Now," *Cureus* 15, no. 2 (2023): e35154, https://doi.org/10.7759/cureus.35154.

3. G. Cottarel and J. Wierzbowski, "Combination Drugs, an Emerging Option for Antibacterial Therapy," *Trends in Biotechnology* 25, no. 12 (2007): 547–555, https://doi.org/10.1016/j.tibtech.2007.09.004.

4. N. Maghradze, "Molecular Epidemiology of " Mycobacterium tuberculosis" in the Country of Georgia: University_of_Basel_Associated_Institution," (2024), https://doi.org/10.1128/spectrum.02181-24.

5. S. Sharma, A. Chauhan, A. Ranjan, et al., "Emerging Challenges in Antimicrobial Resistance: Implications for Pathogenic Microorganisms, Novel Antibiotics, and Their Impact on Sustainability," *Frontiers in Microbiology* 15 (2024): 1403168, https://doi.org/10.3389/fmicb.2024.1403168.

6. P. J. Vanavi, "Study on Impurity Profiling and Characterization of Major Degradation Products for Selected Anti-Tuberculosis Drugs: Maharaja Sayajirao University of Baroda (India)," (2022).

7. M. Małkowski, A. Chudek, A. Almgren-Rachtan, J. T. Chudek, and P. L. Chłosta, "Impact of Fixed-Dose Combination Versus Single-Component Therapy for Benign Prostatic Hyperplasia-Related Urinary Symptoms on Persistence, Adherence, and Satisfaction in a Real-Life Setting," *Pharmaceuticals* 18, no. 10 (2025): 1439, https://doi.org/10.3390/ph18101439.

8. T. A. D. Okaecwe, *Combined First Line Anti-TB Drugs: New Insights Into Stability* (North-West University (South-Africa), 2019).

9. G. S. Burle, P. R. Kakullamarri, S. B. Kothamasu, S. D. M. Kallam, and A. Bodapati, "Case Study on Regulatory Approaches for New Degradation Impurity Exceeding ICH Thresholds in Solubilized Ibuprofen Capsules During Stability Testing," *Journal of International Research in Medical and Pharmaceutical Sciences* 19, no. 3 (2024): 70–82, https://doi.org/10.56557/jirmeps/2024/v19i38936.

10. P. R. Chellini, E. B. Lages, P. H. Franco, F. H. Nogueira, I. C. César, and G. A. Pianetti, "Development and Validation of an HPLC Method for Simultaneous Determination of Rifampicin, Isoniazid, Pyrazinamide, and Ethambutol Hydrochloride in Pharmaceutical Formulations," *Journal of AOAC International* 98, no. 5 (2015): 1234–1239, https://doi.org/10.5740/jaoacint.14-237.

11. M. Oliveira, P. Chellini, and T. Amorim, "Simultaneous Determination of Rifampicin, Isoniazid, Pyrazinamide and Ethambutol in Fixed-Dose Combination Antituberculosis Pharmaceutical Formulations: A Review," *Analytical Methods* 10, no. 10 (2018): 1103–1116, https://doi.org/10.1039/C7AY02686B.

12. S. Khoiri, S. Martono, and A. Rohman, "Optimisation and Validation of HPLC Method for Simultaneous Quantification of Rifampicin, Isoniazid, Pyrazinamide, and Ethambutol Hydrochloride in Anti-Tuberculosis 4-FDC Tablet," *Jurnal Teknologi (Sciences & Engineering)* 77, no. 1 (2015), https://doi.org/10.11113/jt.v77.3870.

13. M. A. Hagga and S. Sultana, "A Novel Quantitative Method for the Simultaneous Assay of Rifampicin (RIF), Isoniazid (INH), Ethambutol (EMB), and Pyrazinamide (PYP) in 4-FDC Tablets," *Oriental Journal of Chemistry* 32 (2016): 3081–3087, https://doi.org/10.13005/ojc/320629.

14. B. Rajeswari, N. Saritha, and N. Devanna, "Method Development and Validation for the Simultaneous Estimation of Ethambutol and Isoniazid by Using RP-HPLC," *Research Journal of Life Sciences, Bioinformatics, Pharmaceutical and Chemical Sciences* 6 (2020): 24–35, https://doi.org/10.26479/2020.0602.02.

15. A. Memon and N. Memon, "Development and Validation of a Simple and Sensitive RP-HPLC Method for Determination of Rifampicin in Bulk and Tablets," *Sindh University Research Journal-SURJ (Science Series)* 49, no. 1 (2017).

16. M. F. Khan, S. A. Rita, and M. S. Kayser, "Theoretically Guided Analytical Method Development and Validation for the Estimation of Rifampicin in a Mixture of Isoniazid and Pyrazinamide by UV Spectrophotometer," *Frontiers in Chemistry* 5 (2017): 27, https://doi.org/10.3389/fchem.2017.00027.

17. S. Vilvamani, S. Mahalingam, S. Nhavilthodi, D. Murugesan, and S. M. Jeyakumar, "Development and Validation of a Simple High-Pressure Liquid Chromatography-Ultraviolet Detection Method for Simultaneous Quantitation of First-Line Anti-Tuberculosis Drugs in Formulations of Fixed-Dose Combination," *Journal of Chromatographic Science* 62, no. 9 (2024): 821–828, https://doi.org/10.1093/chromsci/bmae023.

18. M. R. Yowaraj, S. Vilvamani, T. Bharathiraja, et al., "Pharmacokinetic Drug-Drug Interaction Between First-Line Anti-TB and Anti-Diabetic Drugs in Patients With Tuberculosis and Diabetes Mellitus," supplement, Indian Journal of Tuberculosis 72 (2025): S43–S49, https://doi.org/10.1016/j.ijtb.2024.10.009.

19. M. Sturkenboom, H. van der Lijke, E. Jongedijk, et al., "Quantification of Isoniazid, Pyrazinamide and Ethambutol in Serum Using Liquid Chromatography-Tandem Mass Spectrometry," *Journal of Applied Bioanalysis* 1, no. 3 (2015): 89–98, https://doi.org/10.17145/jab.15.015.

20. S. H. Song, S. H. Jun, K. U. Park, et al., "Simultaneous Determination of First-Line Anti-Tuberculosis Drugs and Their Major Metabolic Ratios by Liquid Chromatography/Tandem Mass Spectrometry," *Rapid Communications in Mass Spectrometry* 21, no. 7 (2007): 1331–1338, https://doi.org/10.1002/rcm.2961.

21. K. H. Hee, J. J. Seo, and L. S. Lee, "Development and Validation of Liquid Chromatography Tandem Mass Spectrometry Method for Simultaneous Quantification of First Line Tuberculosis Drugs and Metabolites in Human Plasma and Its Application in Clinical Study," *Journal of Pharmaceutical and Biomedical Analysis* 102 (2015): 253–260, https://doi.org/10.1016/j.jpba.2014.09.019.

22. D. Fage, R. Brilleman, G. Deprez, M.-C. Payen, and F. Cotton, "Development, Validation and Clinical Use of a LC-MS/MS Method for the Simultaneous Determination of the Nine Main Antituberculosis Drugs in Human Plasma," *Journal of Pharmaceutical and Biomedical Analysis* 215 (2022): 114776, https://doi.org/10.1016/j.jpba.2022.114776.

23. Y. Shen, J. Zhang, Q. Zhang, et al., "Comparative Analysis of Impurity Profiles in Rifampicin Capsules With Different Crystal Forms Using LC-MS/MS," *Journal of Chromatography A* 1746 (2025): 465769, https://doi.org/10.1016/j.chroma.2025.465769.

24. H. Bhutani, S. Singh, K. Jindal, and A. K. Chakraborti, "Mechanistic Explanation to the Catalysis by Pyrazinamide and Ethambutol of Reaction Between Rifampicin and Isoniazid in Anti-TB FDCs," *Journal of Pharmaceutical and Biomedical Analysis* 39, no. 5 (2005): 892–899, https://doi.org/10.1016/j.jpba.2005.05.015.

25. R. M. Beteck, R. Seldon, A. Jordaan, et al., "Quinolone-Isoniazid Hybrids: Synthesis and Preliminary In Vitro Cytotoxicity and Anti-Tuberculosis Evaluation," *MedChemComm* 10, no. 2 (2019): 326–331, https://doi.org/10.1039/C8MD00480C.

26. L. Marcellos, A. Faria, M. Souza, et al., "Simultaneous Analysis of First-Line Anti-Tuberculosis Drugs in Tablets by UV Spectrophotometry Compared to Capillary Zone Electrophoresis," *Open Chemistry* 10, no. 6 (2012): 1808–1816, https://doi.org/10.2478/s11532-012-0102-6.

27. L. M. Duarte, T. L. Amorim, P. R. Chellini, L. H. C. Adriano, and M. A. L. de Oliveira, "Sub-Minute Determination of Rifampicin and Isoniazid in Fixed Dose Combination Tablets by Capillary Zone Electrophoresis With Ultraviolet Absorption Detection," *Journal of Separation Science* 41, no. 24 (2018): 4533–4543, https://doi.org/10.1002/jssc.201800673.

28. H. Acharya and R. Kotadiya, "Analytical Technique Advances for Recently Approved Fixed-Dose Combination of Dapagliflozin and Teneligliptin Hydrobromide Hydrate," *Separation Science Plus* 8, no. 1 (2025): e202400208, https://doi.org/10.1002/sscp.202400208.

29. R. Jain, S. K. Dubey, and G. Singhvi, "Stability Indicating Validated High-Performance Liquid Chromatography Method for Simultaneous Estimation of Chlorin e6 and Curcumin in Bulk and Drug-Loaded Lipidic Nanoformulation," *Separation Science Plus* 6, no. 1 (2023): 2200107, https://doi.org/10.1002/sscp.202200107.

30. B. Glass, S. Agatonovic-Kustrin, Y.-J. Chen, and M. Wisch, "Optimization of a Stability-Indicating HPLC Method for the Simultaneous Determination of Rifampicin, Isoniazid, and Pyrazinamide in a Fixed-Dose Combination Using Artificial Neural Networks," *Journal of Chromatographic Science* 45, no. 1 (2007): 38–44, https://doi.org/10.1093/chromsci/45.1.38.

31. N. B. Chilamakuru, A. D. Vn, N. Pallaprolu, et al., "New Synergistic Benzoquinone Scaffolds as Inhibitors of Mycobacterial Cytochrome bc1 Complex to Treat Multi-Drug Resistant Tuberculosis," *European Journal of Medicinal Chemistry* 272 (2024): 116479, https://doi.org/10.1016/j.ejmech.2024.116479.

32. P. R. Chellini, T. O. Mendes, P. H. Franco, et al., "Simultaneous Determination of Rifampicin, Isoniazid, Pyrazinamide and Ethambutol in 4-FDC Tablet by Raman Spectroscopy Associated to Chemometric Approach," *Vibrational Spectroscopy* 90 (2017): 14–20, https://doi.org/10.1016/j.vibspec.2017.03.001.

33. R. E. Tarigan, E. L. F. Mendrofa, and C. Surbakti, "Simultaneous Determination of Isoniazid and Pyridoxine Hydrochloride in Tablet Dosage Forms Using Ratio Subtraction Spectrophotometry," *Jurnal Kimia Dan Pendidikan Kimia* 9, no. 1 (2024): 1–14, https://doi.org/10.20961/jkpk.v9i1.78154.

34. F. Patel, R. Kotadiya, R. Patel, and M. Patel, "Development and Validation of a New Reversed Phase HPLC Method for the Quantitation of Azithromycin and Rifampicin in a Capsule Formulation," *Journal of Chromatographic Science* 62, no. 8 (2024): 742–750, https://doi.org/10.1093/chromsci/bmae006.

Supporting Information

Additional supporting information can be found online in the Supporting Information section.

Supporting File:sscp70181-sup-0001-SuppMat.docx.